



Cite this: *Polym. Chem.*, 2020, **11**, 3195

## Surfactant-free synthesis of layered double hydroxide-armored latex particles†

X. G. Qiao,<sup>a,b</sup> P.-Y. Dugas,<sup>a</sup> V. Prevot<sup>\*c</sup> and E. Bourgeat-Lami  

MgAl-layered double hydroxide (LDH)-armored latexes were produced by Pickering emulsion polymerization of styrene (St) using 2-hydroxyethyl methacrylate (HEMA) and methyl methacrylate (MMA) as auxiliary comonomers. While St led to bare polymer latex particles, St/HEMA and St/MMA mixtures produced nanocomposite latexes. Clearly, the use of hydrophilic comonomers such as HEMA or MMA is key to promoting adhesion of the LDH nanoplatelets onto the polymer particle surface and latex stabilization. Several parameters such as the nature and amount of auxiliary comonomer, the ionic strength and the LDH percentage were shown to play a crucial role in the formation and stability of the resulting MgAl-LDH-armored particles. Increasing the HEMA content above 8 wt% (based on total monomer) induced aggregation of both the LDH and latex particles, which was tentatively attributed to HEMA hydrolysis under basic conditions. Similar results were observed for MMA although destabilization occurred for higher concentrations (*i.e.*, >30 wt%). Transmission electron microscopy confirmed the armored morphology with the concomitant presence of excess of free-standing platelets for high LDH contents. The average particle diameter was strongly dependent on the synthesis conditions and decreased with increasing the amount of MMA and/or the LDH content, indicating that the inorganic particles effectively played the role of a Pickering stabilizer. The addition of salt screened the positive charges between adjacent LDH sheets allowing closer packing of the LDH platelets onto the latex particle surface. The higher the salt content in the polymerization medium, the larger was the size of the nanocomposite particles.

Received 27th January 2020,  
Accepted 9th April 2020

DOI: 10.1039/d0py00140f

[rsc.li/polymers](http://rsc.li/polymers)

## Introduction

Emulsion polymerization is a widespread process for the production of polymer colloids in aqueous dispersed media, also known as synthetic latexes. The resulting materials can be used in many different applications including coatings, adhesives and biomedicine. Polymer latexes are most often prepared in the presence of molecular surfactants that play an important role in controlling the particle size, the reaction rate and latex stability. However, one of the major drawbacks of surfactants used in emulsion polymerization, is their ability to migrate and accumulate at the film surface or at the film/substrate interface, which may degrade the coating properties.<sup>1</sup> In

recent years, various strategies have been implemented to address this issue such as the use of reactive surfactants that are covalently bound to the particle surface, *in situ* self-assembly of block copolymers,<sup>2</sup> and the synthesis of Pickering latexes that can be described as polymer particles stabilized by inorganic solids.<sup>3</sup> In this last strategy, molecular surfactants are replaced by inorganic particles that adsorb at the polymer particle surface, playing the role of stabilizer.<sup>4</sup> The corresponding process is known as Pickering emulsion polymerization, by analogy with the stabilization of emulsions by solid particles first described by Ramsden<sup>5</sup> and Pickering.<sup>6</sup> The formation of an inorganic armor around the polymer latex particles can additionally be exploited to create ordered structures with the inorganic particles located at the boundaries between the polymer particles, leading to film materials with improved optical,<sup>7</sup> barrier<sup>8,9</sup> or mechanical properties.<sup>10–13</sup> It is noteworthy that although Pickering emulsion polymerization is often confused with the polymerization of Pickering emulsions,<sup>14,15</sup> both processes are very different from the mechanistic point of view.

Until now, a large variety of inorganic nanoparticles has been investigated as solid stabilizers in Pickering emulsion polymerization, such as colloidal silicas,<sup>16–22</sup> LAPONITE® clay discs,<sup>4,9,23–27</sup> iron oxide nanoparticles,<sup>28,29</sup> zinc oxide,<sup>30,31</sup>

<sup>a</sup>Univ Lyon, Université Claude Bernard Lyon 1, CPE Lyon, CNRS, UMR 5265, Chemistry, Catalysis, Polymers and Processes (C2P2), 43 Bd. du 11 Novembre 1918, F-69616 Villeurbanne, France. E-mail: elodie.bourgeat-lami@univ-lyon1.fr

<sup>b</sup>Henan Joint International Research Laboratory of Living Polymerizations and Functional Nanomaterials, Henan Key Laboratory of Advanced Nylon Materials and Application, School of Materials Science and Engineering, Zhengzhou University, Zhengzhou 450001, China

<sup>c</sup>Université Clermont Auvergne, CNRS, SIGMA Clermont, ICCF, F-63000 Clermont-Ferrand, France. E-mail: vanessa.prevot@uca.fr

† Electronic supplementary information (ESI) available. See DOI: 10.1039/d0py00140f



cerium dioxide<sup>7</sup> and titania.<sup>32–35</sup> To promote the effective adsorption of the Pickering stabilizer onto the polymer latex particles, several strategies have been reported. For example, Percy *et al.*<sup>16</sup> used 4-vinylpyridine (4VP) as an auxiliary comonomer to form polymer/silica composite particles with a raspberry-like morphology, taking advantage of the strong acid–base interaction between 4VP and silica. 2-Vinylpyridine (2VP)<sup>20</sup> and 1-vinylimidazole<sup>18</sup> also served a similar purpose. Alternatively, cationic monomers or cationic initiators such as 2-(methacryloyl) ethyltrimethylammonium chloride<sup>19</sup> and 2,2'-azobis(2-methylpropionamide) dihydrochloride (V50)<sup>20</sup> were used to synthesize silica-based poly(methyl methacrylate) (PMMA) or P2VP composite particles, thanks to their ability to strongly interact electrostatically with the surface of the inorganic particles. Xu *et al.*<sup>28</sup> also reported the successful formation of magnetic polystyrene (PSt) microspheres using V50 as cationic initiator and poly(methacrylic acid) (PMAA)-functionalized iron oxide (IO) nanoparticles as Pickering stabilizer. Electrostatic interaction between the amidine group of V50 and the carboxylate anions of PMAA under basic conditions was key in obtaining stable composite particles with the targeted raspberry-like morphology. Our group also recently described the surfactant-free synthesis of composite latex particles with a patchy IO overlayer through Pickering emulsion polymerization of St and (meth)acrylates, using (meth)acrylic acids (MAA or AA) as auxiliary comonomers.<sup>29</sup> A minimum amount of auxiliary comonomer was required to favor IO adsorption at the latex particle surface, while a too high concentration promoted IO aggregation and latex destabilization. Other workers reported the use of poly(ethylene glycol)-based macromonomers (PEGMA or Sipomer PAM) to favor adsorption of silica<sup>21</sup> or LAPONITE® clay platelets<sup>9,23</sup> at the surface of Pickering latex particles. In the particular case of clay minerals, other examples of auxiliary comonomers include MAA,<sup>24</sup> methyl acrylate,<sup>9</sup> and methyl methacrylate (MMA).<sup>24</sup> The concentration of the latter must be however carefully adjusted as a too high amount of MMA promotes latex destabilization due to substantial hydrolysis of this monomer under basic conditions as shown by Teixeira *et al.*<sup>24</sup> for LAPONITE® clay.

Among the different inorganic fillers of interest for colloidal nanocomposites, layered double hydroxides (LDHs), have gained increasing attention due to their 2-dimensional morphology and their tunable chemical composition.<sup>36–38</sup> LDHs display a brucite like structure in which a fraction of the divalent metal cations is replaced by trivalent cations. Such substitution leads to a positive charge at the layer surface compensated by the intercalation of anions into the interlayer space. Compared to clay minerals, LDH matrices possess specific intrinsic properties such as anionic exchange, highly hydroxylated layers and biocompatibility, of great interest in various applications including catalysis, biology or coatings.<sup>39,40</sup> The synthesis of LDH-armored latex particles by Pickering emulsion polymerization could be an alternative way to obtain efficient dispersions of LDH platelets into polymer matrices and create new smart functional nanocomposite materials. Even if several authors have reported the formation of

Pickering emulsions stabilized by LDH particles,<sup>41–44</sup> to the best of our knowledge no previous research has investigated the use of LDHs as Pickering stabilizers in emulsion polymerization. A few years ago, Qiu and Qu<sup>45</sup> reported the surfactant-free emulsion polymerization of styrene (St) in the presence of LDH platelets using potassium persulfate as thermal initiator to favor polymer intercalation into the LDH galleries, but no evidence of formation of LDH/PSt composite particles was provided in this article.

In the present work, we report Pickering emulsion polymerization of St stabilized by  $Mg_3Al(OH)_8(CO_3)_{0.5}$  LDH nanosheets. Aiming at preparing LDH-armored composite particles, 2-hydroxyethyl methacrylate (HEMA) and MMA were investigated as auxiliary comonomers to promote adhesion of the LDH platelets onto the surface of the polymer latex particles. The effect of the nature and concentration of the auxiliary comonomers, the ionic strength, and the LDH content on particle morphology and polymerization kinetics was investigated in details to provide insights into the mechanism of formation of the Pickering latex particles.

## Experimental

### Materials

Aluminum nitrate ( $Al(NO_3)_3$ , >97%), aluminum chloride ( $AlCl_3$ , >97%), magnesium nitrate ( $Mg(NO_3)_2$ , >97%), magnesium chloride ( $MgCl_2$ , >97%), zinc nitrate ( $Zn(NO_3)_2$ , >99%), zinc chloride ( $ZnCl_2$ , >98%), potassium nitrate ( $KNO_3$ , >99%), potassium chloride ( $KCl$ , >98%), sodium chloride ( $NaCl$ , ≥99.5%) and sodium hydroxide ( $NaOH$ , >98%) were all purchased from Sigma-Aldrich, and used without further purification. The monomers, styrene (St, 99%, Acros), methyl methacrylate (MMA, 99%, Acros), methacrylic acid (MAA, ≥ 99.5%, Acros), and 2-hydroxyethyl methacrylate (HEMA, 99%, Aldrich) were used as received. 2,2'-Azobis[2-(2-imidazolin-2-yl)propane] (ADIBA, Wako Chemicals GmbH) was used as the initiator. All experiments were performed in deionized water (Purelab Classic UV, ElgaLabWater).

### Syntheses

$Mg_3Al(OH)_8(CO_3)_{0.5}$ . The LDH platelets noted hereafter MgAl-LDH were synthesized by flash precipitation in water followed by hydrothermal treatment as previously reported.<sup>46</sup> Typically, 500 mL of a 0.1 M mixture of  $Mg(NO_3)_2 \cdot 6H_2O$  and  $Al(NO_3)_3 \cdot 9H_2O$  ( $Mg/Al = 3$ ) was prepared, and the pH of the solution was adjusted to 10.0 by rapid addition of  $NaOH$  (0.2 M). After further stirring for 30 min, the precipitate was centrifuged and washed twice before being transferred into a Teflon-lined stainless steel autoclave and submitted to an hydrothermal treatment at 150 °C for 4 hours.

*Pickering emulsion polymerization* of St in the presence of MgAl-LDH nanoparticles was performed in a 25 mL three-necks round-bottom flask equipped with a mechanical stirrer (overhead, teflon turbine blade, 500 rpm), a condenser and a nitrogen inlet. In a typical experiment (entry H02 in Table 1),



the initiator: ADIBA (0.01 g) and LDH (0.1 g, weighted according to the solids content of the LDH colloidal suspension) were first introduced in deionized water (9.0 g, including the water in the weighted LDH colloidal suspension) and stirred under nitrogen bubbling for 20 min in an ice bath. The mixture was then transferred into the flask, which was immersed into an oil bath thermostated at 70 °C. Once the temperature reached 60 °C, the monomers, a mixture of styrene and the auxiliary comonomer (either HEMA or MMA) (total = 1.0 g) were introduced in the suspension to start polymerization. Samples were periodically withdrawn to follow monomer conversion by gravimetric analysis and the particle diameter by dynamic light scattering (DLS). The experimental conditions and main characteristics of the resulting latex particles are listed in Tables 1–4.

## Characterizations

X-ray diffraction (XRD) was performed on a PANalytical X'Pert Pro diffractometer equipped with an X'Celerator Scientific detector and a Cu anticathode ( $K\alpha 1/K\alpha 2$ ). The diffracted beam was detected over a range of 3°–70° ( $2\theta$ ) with a step size of 0.0167° and a counting time of 350 s per step. The density of the LDH powder was measured using an AccuPyc Pycnometer II 1340 (Micromeritics) with helium as density medium. Dynamic light scattering (DLS, Nano ZS from Malvern Instruments) was used to measure the particle size (average hydrodynamic diameter,  $Z_{av.}$ ) and the dispersity of the samples (PDI, the higher this value, the broader the size distribution). The data were collected at 173° using the fully automatic mode of the zetasizer system and the cumulants analysis method. Zeta potential ( $\zeta$ ) measurements were carried out on the same

**Table 1** Experimental conditions and characteristics of the latex particles synthesized by Pickering emulsion copolymerization of St and HEMA for various HEMA and MgAl-LDH contents<sup>a</sup>

No.	St/HEMA (g/g)	LDH (g)	Conversion (wt%)	$Z_{av.}$ (DLS) (nm)	PDI (DLS)	$D_n$ (TEM) (nm)	$D_w/D_n$	$N_{LDH}/N_{latex}$
St1 <sup>b</sup>	1.0/0	0.1	41.9	361	0.09	333	1.01	198
H01 <sup>c</sup>	0.92/0.08	0	98.0	243	0.04	210	1.01	0
H02	0.96/0.04	0.1	80.9	183	0.04	130	1.04	6
H03	0.94/0.06	0.1	86.4	208	0.11	141	1.06	7
H04	0.92/0.08	0.1	98.2	233	0.12	145	1.18	7
H05 <sup>d</sup>	0.88/0.12	0.1	91.0	—	—	196	1.45	18
H06	0.92/0.08	0.025	86.6	526	0.26	134	1.08	1.5
H07	0.92/0.08	0.05	90.6	300	0.58	120	1.09	2

<sup>a</sup> Water = 9 g and ADIBA = 0.01 g. <sup>b</sup> Control experiment performed in the presence of 10 wt% of LDH using St as the sole monomer. <sup>c</sup> Control experiment performed in the presence of 8 wt% HEMA and in the absence of clay (the pH was fixed at 10.2). <sup>d</sup> Unstable latex. The final product was however characterized by gravimetry to determine the monomer conversion and by TEM after glass-wool filtration to evaluate the particle size and morphology.

**Table 2** Experimental conditions and characteristics of the latex particles synthesized by Pickering emulsion polymerization of St in the presence of 10 wt% of MgAl-LDH (based on total monomer) using increasing amounts of MMA as auxiliary comonomer<sup>a</sup>

No.	St/MMA (g/g)	Conversion (%)	$Z_{av.}$ (DLS) (nm)	PDI (DLS)	$D_n$ (TEM) (nm)	$D_w/D_n$ (TEM)	$N_{LDH}/N_{latex}$
M01	0.9/0.1	84.9	177	0.05	131	1.03	6
M02	0.8/0.2	86.8	181	0.11	122	1.02	5
M03	0.7/0.3	94.0	367	0.53	117	1.05	4
M04 <sup>b</sup>	0.6/0.4	45	—	—	—	—	—
M05 <sup>b</sup>	0.5/0.5	—	—	—	—	—	—
M06 <sup>b</sup>	0/1.0	—	—	—	—	—	—

<sup>a</sup> Water = 9 g, ADIBA = 0.01 g and MgAl-LDH = 0.1 g. <sup>b</sup> Latex destabilization in the course of the polymerization.

**Table 3** Experimental conditions and characteristics of the latex particles synthesized by Pickering emulsion copolymerization of St and MMA (80/20 wt/wt) in the presence of increasing amounts of MgAl-LDH<sup>a</sup>

No	St/MMA (g/g)	LDH (g)	Conversion (%)	$Z_{av.}$ (DLS) (nm)	PDI (DLS)	$D_n$ (TEM) (nm)	$D_w/D_n$ (TEM)	$N_{LDH}/N_{latex}$
M07	0.8/0.2	0	64.9	242	0.02	210	1.01	0
M08	0.8/0.2	0.025	65.7	201	0.03	174	1.03	4
M09	0.8/0.2	0.050	75.2	166	0.01	142	1.03	4
M10	0.8/0.2	0.075	75.6	163	0.05	131	1.02	5
M02	0.8/0.2	0.1	86.8	181	0.11	122	1.05	5

<sup>a</sup> Water = 9 g, total monomer = 1 g and ADIBA = 0.01 g.



**Table 4** Experimental conditions and characteristics of the latex particles synthesized by Pickering emulsion copolymerization of St and MMA (90/10 wt/wt) in the presence of 10 wt% (based on total monomer) of MgAl-LDH and increasing salt concentrations<sup>a</sup>

No	NaCl (mM)	Conversion (%)	$Z_{\text{av.}}$ (DLS) (nm)	PdI (DLS)	$D_n$ (TEM) (nm)	$D_w/D_n$ (TEM)	$N_{\text{clay}}/N_{\text{latex}}$
M01	0	84.9	177	0.05	131	1.03	6
M11	2	63.4	217	0.015	184	1.06	22
M12	10	49.3	240	0.006	211	1.02	42
M13 <sup>b</sup>	50	30.5	385	0.125	275	1.04	152

<sup>a</sup> Water = 9 g, total monomer = 1 g, ADIBA = 0.01 g and MgAl-LDH = 0.1 g. <sup>b</sup> Latex destabilization after 24 hours.

instrument using a dilute LDH dispersion (50 mg L<sup>-1</sup>) containing 1 mM KNO<sub>3</sub> to adjust the ionic strength. AFM images were obtained on a Bruker Nanoscope IIIa atomic force microscope. Imaging was achieved using the repulsive mode in intermittent contact, commonly known as the “tapping” mode. For imaging the LDH particles, a drop of a dilute dispersion was casted on a freshly cleaved mica substrate with scotch tape. Transmission electron microscopy (TEM) was performed at an accelerating voltage of 80 kV with a Philips CM120 transmission electron microscope (Centre Technologique des Microstructures (CTμ), plate-forme de l'Université Claude Bernard Lyon 1, Villeurbanne, France). Highly diluted samples were dropped on a Formvar-carbon coated copper grid and dried under air. The number and weight average particle diameters ( $D_n$  and  $D_w$ , respectively) and the polydispersity index

( $D_w/D_n$ ) were calculated using  $D_n = \sum n_i D_i / \sum n_i$  and  $D_w = \sum n_i D_i^4 / \sum n_i D_i^3$ , where  $n_i$  is the number of particles with diameter  $D_i$ . The percentage of latex surface coverage by the LDH platelets was determined as previously reported in the literature assuming a 2D square lateral packing of the LDH discs, and using the number-average particle diameter determined by TEM (see the ESI† for more details).<sup>24</sup>

## Results and discussion

### LDH synthesis

A colloidal suspension of MgAl-LDH nanoparticles (solids content = 2.95 wt%, pH = 10.2) was prepared following a fast coprecipitation strategy combined with a subsequent hydro-

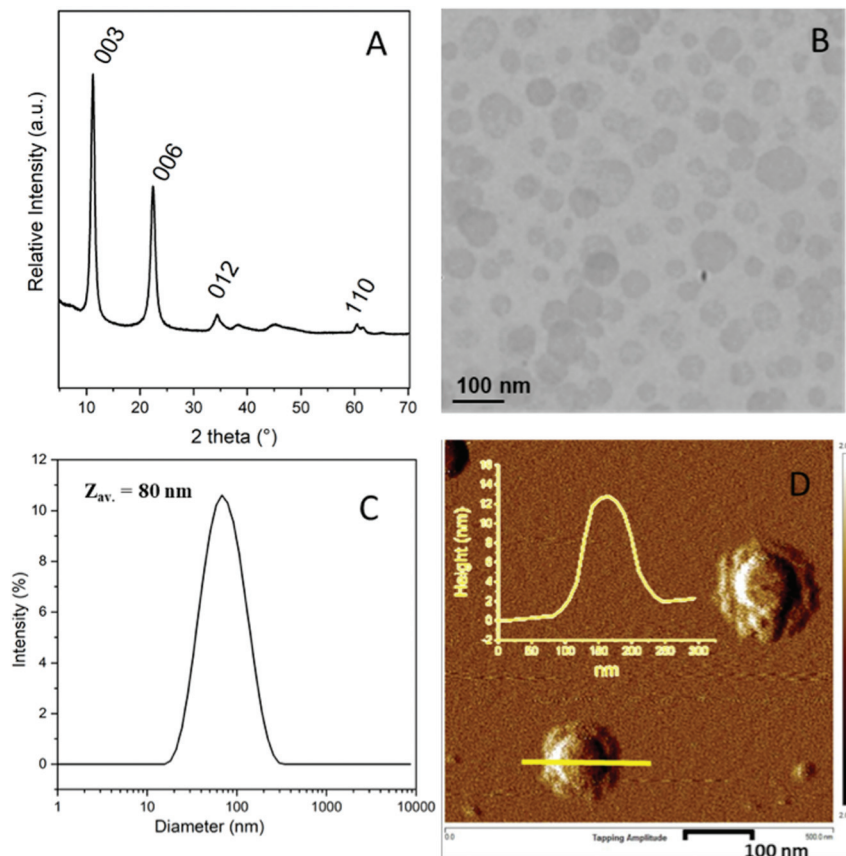


**Fig. 1** MgAl-LDH nanoparticles. (A) Powder X-ray diffraction pattern, (B) TEM image, (C) DLS measurement and (D) AFM phase image with, in the inset, the height profile of a LDH particle.



thermal treatment. The resulting nanoparticles displayed a characteristic LDH structure as evidenced by powder X-ray diffraction (Fig. 1A). The pattern is typical of a well-crystallized sample and exhibits at low angle, two intense diffraction peaks corresponding to (003) and (006) reflections confirming the hydrotalcite lamellar structure, and two smaller peaks at higher angle, assigned to (012) and (110) reflections. The positions of the  $00l$  diffraction lines indicate an interlamellar distance of 0.76 nm, consistent with the presence of carbonate

anions in the interlayer domain.<sup>47</sup> TEM analysis showed the formation of platelet-like particles with a particle size in the range of 10 to 100 nm in agreement with DLS analysis ( $Z_{av.} = 80$  nm, PDI = 0.25) (Fig. 1B and C, respectively). The LDH platelets displayed an average thickness of  $10 \pm 4$  nm as determined by AFM (Fig. 1D) and a density of  $2.0 \text{ g cm}^{-3}$ . A zeta potential value ( $\zeta$ ) of  $+31 \text{ mV}$  ( $\pm 5 \text{ mV}$ ) was measured at pH 9.3 on a very dilute dispersion, evidencing as expected the positive surface charge properties of MgAl-LDH particles.  $\zeta$  values remained positive in a wide range of pH (from pH = 4.5 to 13) corresponding to the stability range of LDH suspensions (Fig. S1, ESI†).

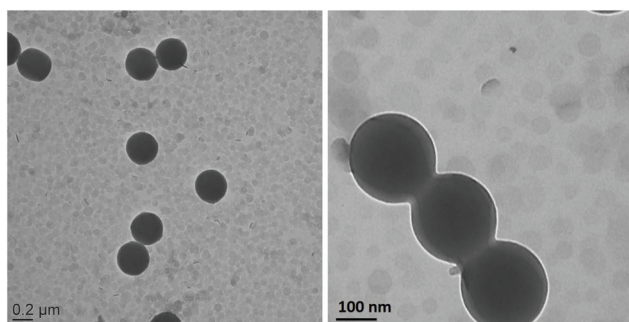


**Fig. 2** TEM images of PSt latex particles synthesized in the presence of MgAl-LDH nanoparticles at low and high magnification, showing the absence of interaction between the two populations of particles (St1 in Table 1).

### Synthesis of LDH-armored latexes

The objective of the present work was to synthesize composite latex particles armored with a layer of LDH platelets by surfactant-free emulsion polymerization. Previous works on Pickering emulsion polymerization using various types of inorganic nanoparticles, have shown that latex stability and final particle morphology strongly depend on the physicochemical properties of the mineral and the nature and composition of the monomer mixture.<sup>29</sup> According to Lotierzo *et al.*,<sup>22</sup> inorganic particles do not spontaneously adsorb onto the surface of latex particles in the absence of external attractive forces. The authors argued instead that oligoradicals formed

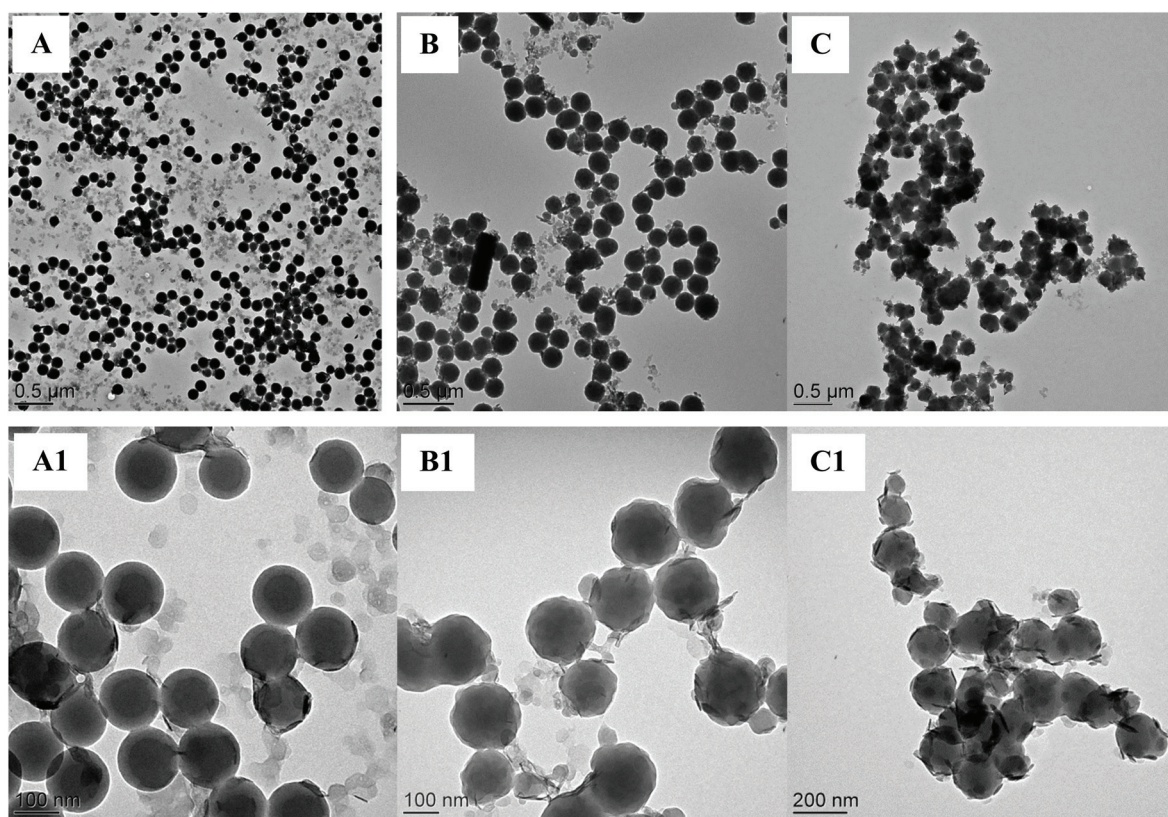


**Fig. 3** TEM images of LDH/polymer composite particles obtained by Pickering emulsion copolymerization of St and HEMA in the presence of 10 wt% of LDH (based on total monomer) for increasing HEMA contents: (A and A1) 4.0 wt%, (B and B1) 8.0 wt% and (C and C1) 12.0 wt%, based on total monomer (runs H02, H04 and H05 in Table 1).



in the early stages of the polymerization need to be trapped at the inorganic particles surface to change their wetting properties, allowing subsequent adhesion of the inorganic solid on the latex surface *via* heterocoagulation. In other words, the growing oligoradicals must have a certain affinity for the mineral surface to promote interfacial adsorption. This is usually achieved by using initiators and/or monomers displaying favorable interactions with the inorganic particles.

To test this assumption, we conducted a control experiment using styrene as the sole monomer (St1 in Table 1). The TEM images of Fig. 2 clearly show a mixture of bare polymer latex particles (around 330 nm in diameter) and free LDH nanosheets that appear as light grey discs, with no affinity between the two populations of particles, which supports the idea that the LDH platelets are too hydrophilic for the polystyryl radicals formed in water to irreversibly adhere to their surface. According to this, in the following two sections HEMA and MMA were investigated as auxiliary comonomers in order to promote the formation of LDH-armored particles.

#### HEMA as auxiliary comonomer

In this section, HEMA was chosen as auxiliary comonomer for the Pickering emulsion polymerization of St in order to enhance the compatibility between the hydrophilic LDH and the hydrophobic PST. Indeed, HEMA is known to hydrolyze under basic conditions to form MAA and ethylene glycol,<sup>48</sup> which may promote electrostatic interaction between the growing oligoradicals and the positively charged LDH surface. We first added HEMA to the LDH suspension and stirred for 30 minutes in order to modify its surface, but the system lost stability once the reaction started after the addition of St. HEMA is indeed known to undergo fast hydrolysis in diluted alkaline solutions even at room temperature.<sup>49</sup> The released MAA molecules have likely interacted with the LDH surface,<sup>50</sup> which promoted LDH aggregation and subsequent latex destabilization. To confirm this assumption, increasing amounts of MAA, with molar concentrations equivalent to the amount of HEMA used in the Pickering emulsion polymerization experiments, were introduced into the LDH suspension. The results are reported in Table S1 (ESI†) and show that the LDH particle size increased with increasing the amount of MAA, indicating that the latter can effectively interact with the sheets surface and induce LDH aggregation. We thus decided to retard the addition of HEMA, and introduce it together with St as described in the experimental part (H02, Table 1). A stable latex with LDH platelets located at the particle surface forming the so-called armored morphology, was indeed obtained by this method using 8 wt% of HEMA with respect to the total amount of monomer (Fig. 3B and B1).

Interestingly, as seen in Table 1, the addition of LDH not only led to armored particles but also had a significant impact on the TEM diameter that decreased from 210 nm without LDH (H01) to 145 nm in the presence of 10 wt% of LDH (H04), for otherwise a fixed HEMA content of 8 wt%, providing clear evidence that the inorganic platelets influenced the particle formation stage and contributed to latex stabilization. LDH

also influenced the polymerization kinetics as can be concluded by comparing the experiments performed without (H01) and with (H04) LDH (Fig. 4). Indeed, the decrease of particle size resulted in a concomitant increase of reaction rate as a direct consequence of the increase of the total number of particles and radical compartmentalization.

**Effect of HEMA content.** The amount of HEMA was next varied from 0.04 g to 0.12 g (*i.e.*, from 4.0 to 12.0 wt% based on total monomer) for a fixed LDH content of 10 wt%, to see its effect on the polymerization kinetics and the final particle size and morphology (H02 to H05 in Table 1).

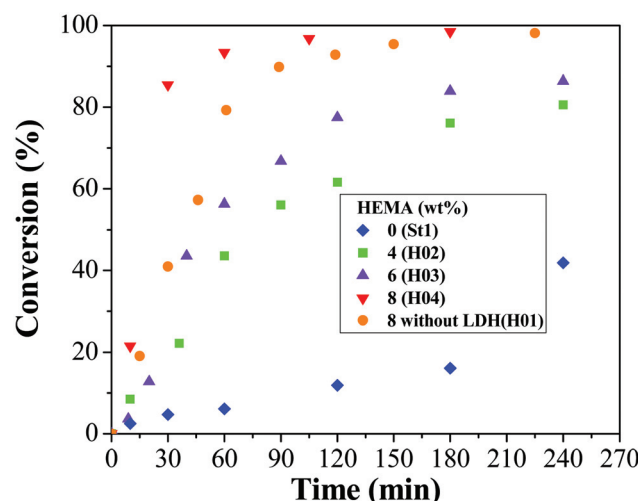


Fig. 4 Effect of HEMA content on the evolution of monomer conversion with time during the Pickering emulsion copolymerization of St and HEMA in the presence of 10 wt% of LDH (based on total monomer). HEMA content = 4.0, 6.0 and 8.0 wt%, based on total monomer. The kinetics of the blank experiment without LDH and 8 wt% of HEMA (H01) is also reported for comparison (see Table 1 for experimental details).

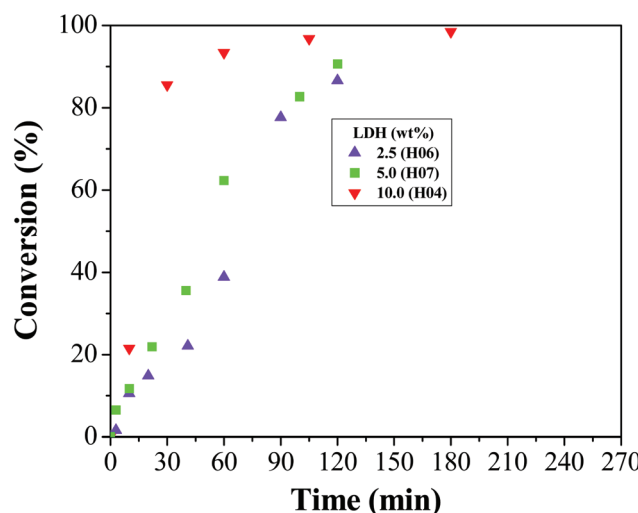


Fig. 5 Overall monomer conversion vs. time during Pickering emulsion copolymerization of St and HEMA (92/8 wt/wt) for different LDH contents (see Table 1 for experimental details).

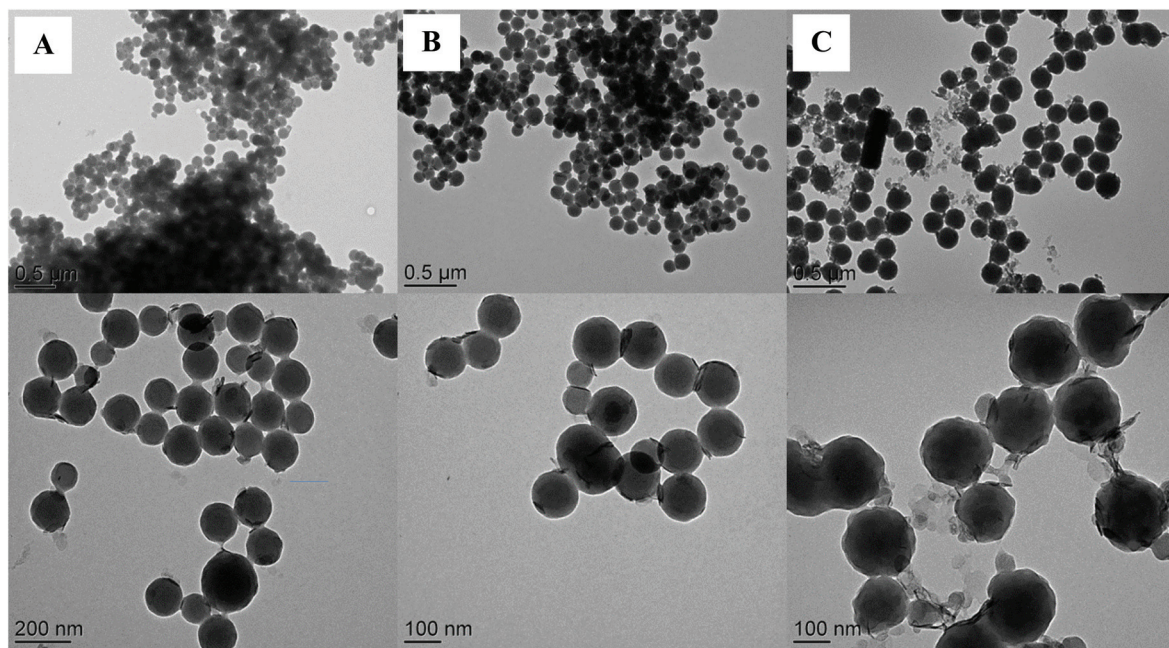


Fig. 4 and Table 1 show that the polymerization rate and the TEM diameter increased with increasing the amount of HEMA from 4 wt% (H02) to 8 wt% (H04) while the latex destabilized at higher concentration (12 wt% of HEMA, H05 in Table 1). The nucleation rate in surfactant-free emulsion polymerization strongly depends on the events taking place in water and notably on the rate of aqueous phase polymerization, which in turns depends on the monomer(s) concentration in water. The addition of HEMA increased the total monomer concentration in water, which increased the polymerization rate. Although all latexes obtained for HEMA contents below 8 wt% were colloidally stable (*i.e.*, there was no massive coagulation observed), the substantial difference in particle size between DLS and TEM analyses (almost 100 nm difference for H04, for instance) and the high PdI values ( $PdI > 0.1$ ) suggest that the particles were slightly aggregated. Fig. 3 shows the TEM images of the corresponding LDH/polymer composite particles. The images clearly show that increasing the HEMA content promoted LDH adsorption on the surface of the latex particles as evidenced by the gradual disappearance of free LDH sheets in the surrounding environment of the Pickering latexes. However in parallel the particle morphology also became more irregular, the LDH platelets adopting a more disordered arrangement at the latex particle surface (Fig. 3C and C1). This is in agreement with the DLS results and also in line with the above observation of LDH aggregation in the presence of HEMA. According to the literature, the hydrolysis of methacrylates is first-order with respect to both the ester and the hydroxyl ions.<sup>51</sup> The hydrolysis rate thus increased with increasing the HEMA concentration leading to both LDH and latex aggregation, explaining the increase in size and irregular morphology of the composite particles for

high HEMA contents, resulting for a too high amount, in latex destabilization.

**Effect of LDH content.** The influence of LDH content was next studied for a fixed HEMA content of 8 wt% (H06, H07 and H04 in Table 1). Fig. 5 shows the evolution of the overall monomer conversion as a function of time for this series of experiments. The polymerization rate increased with increasing the amount of LDH, while in parallel the particle size and the size distribution (as determined by TEM analysis) first decreased and then increased (see Table 1). As an increase in particle size should result in a lower reaction rate, a possible explanation for the higher polymerization rate is that a higher number of primary particles was formed initially with increasing LDH content due to favored nucleation. These unstable primary particles would however coagulate one another during polymerization to reduce the overall interfacial energy of the system leading to larger particles. The extent of aggregation, and therefore the size of the final particles, would then depend on both the hydrolysis rate and the LDH content. On the one hand, increasing the amount of LDH (and thus the number of platelets) increases the probability of heterocoagulation events with a growing oligoradical promoting nucleation, but on the other hand, it also increases the concentration of hydroxyl ions and thus the hydrolysis rate, which may favor hetero-aggregation, resulting in a decrease of the total particle number. This assumption is supported by the TEM image of Fig. 6C (10 wt% of LDH) that shows the formation of particles with a bumpy rough surface.

As shown by TEM, increasing the amount of LDH also led to slight excess of LDH sheets in water, whose proportion was however not quantified. The presence of excess inorganic par-



**Fig. 6** TEM images of LDH/polymer composite particles obtained by Pickering emulsion copolymerization of St and HEMA (St/HEMA = 92/8 wt/wt) in the presence of increasing LDH contents. (A) 2.5 wt%, (B) 5.0 wt% and (C) 10.0 wt%, based on total monomer (runs H06, H07 and H04 in Table 1).



ticles in water has already been reported in the literature for high inorganic/monomer weight ratios, using silica<sup>52</sup> or LAPONITE® clay<sup>9,24</sup> particles as Pickering stabilizer. As seen in Table 1, another noteworthy difference between low and high LDH contents is the average number of LDH platelets per latex particle as determined from their respective diameters and

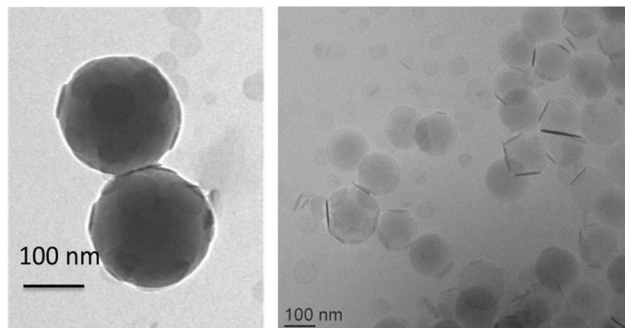


Fig. 7 TEM (left) and cryo-TEM (right) images of LDH/polymer composite latex particles obtained by Pickering emulsion copolymerization of St and MMA (St/MMA = 80/20 wt/wt) in the presence of 10 wt% of LDH (M02 in Table 2). More images can be seen in the ESI (Fig. S3†).

concentrations (details of the calculation are provided in ESI†). The obtained values are particularly low for the lowest LDH contents (on average 1.5 and 2 LDH platelets per latex particle for 2.5 and 5 wt% of LDH, respectively) and more than three times higher for 10 wt% of LDH (around 7, H04). Although, as mentioned above, there is a slight excess of LDH sheets in water for H04, that is not taken into account in the calculation, these values are in reasonable good qualitative agreement with the TEM images, and point to the high stabilizing efficiency of the LDH platelets, which can likely be attributed to their high surface charge density (3.1 charge per nm<sup>2</sup>). Estimation of the percentage of surface coverage of the latex particles by the LDH platelets show that as expected the latex surface coverage increased with increasing LDH content although the calculated values were surprisingly low (see Table S2, ESI†). Such a low surface coverage can likely explain the limited colloidal stability observed for the latex particles synthesized in the presence of 2.5 and 5 wt% of LDH, as attested again by the discrepancy between DLS and TEM diameters and the high PdI values (see Table 1).

In a last experiment, we wanted to determine whether a similar LDH-armored morphology could be obtained by physical blending of LDH sheets and polymer latex particles.

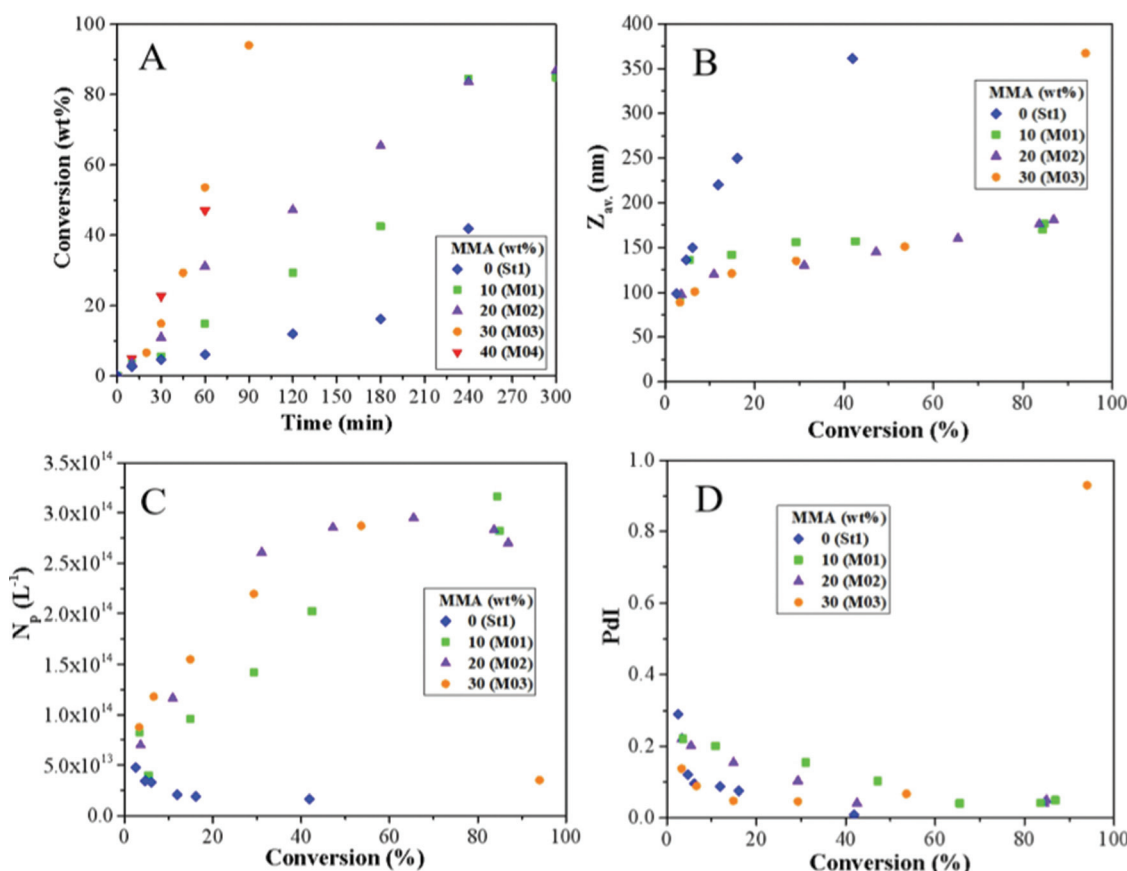


Fig. 8 Effect of MMA content on the evolutions of (A) the overall monomer conversion with time, and of (B) the average particle size ( $Z_{av}$ ), (C) the particle number ( $N_p$ ) and (D) the size dispersity (PdI) with monomer conversion during Pickering emulsion copolymerization of St and MMA in the presence of 10 wt% of LDH (based on total monomer). MMA content = 0, 10, 20, 30 and 40 wt% (based on monomers) (see Table 1 and 2 for experimental details).



For this purpose, an aliquot of LDH stock suspension was added to the surfactant-free latex (H01, Table 1) in the same proportions as in H04, and stirred for one night before characterization by cryo-TEM (Fig. S2, ESI†). It is clear from the images that the LDH platelets did not adhere to the surface of the latex particles indicating that LDH adsorption took place during the polymerization reaction and was thus

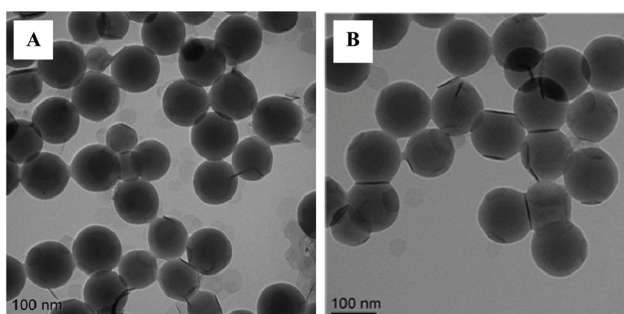


Fig. 9 TEM images of LDH/polymer composite latex particles obtained by Pickering emulsion copolymerization of St and MMA in the presence of 10 wt% of LDH (based on total monomer) for: (A) 10 wt% (M01) and (B) 20 wt% (M02) of MMA (Table 2).

kinetically controlled. We believe that oligoradicals formation at the inorganic particle surface provided the necessary driving force for heterocoagulation, in agreement with previous literature.<sup>22</sup>

### MMA as auxiliary comonomer

In order to minimize hydrolysis of the auxiliary comonomer and improve latex stability, MMA, which is less water soluble than HEMA, was evaluated for the formation of stable P(St-*co*-MMA)/LDH composite latex particles.

TEM analysis of the latex produced in the presence of 20 wt% of MMA and 10 wt% of LDH (based on total monomer, M02 in Table 2) indicated successful formation of LDH-armed particles (Fig. 7). In addition, the particle diameter ( $D_n = 122$  nm, Table 2) was significantly smaller than the diameter of the PSt latex particles synthesized in the same conditions in the absence of MMA ( $D_n = 333$  nm, St1 in Table 1), and also smaller than the diameter of the blank experiment without LDH ( $D_n = 210$  nm, M07 in Table 3). The diminution of the particle size was again accompanied by a concomitant increase of the final monomer conversion (64.9 wt% without LDH (M07, Table 3) vs. 86.8 wt% in the presence of 10 wt% of LDH (M02, Table 2)), as a direct consequence of the increase

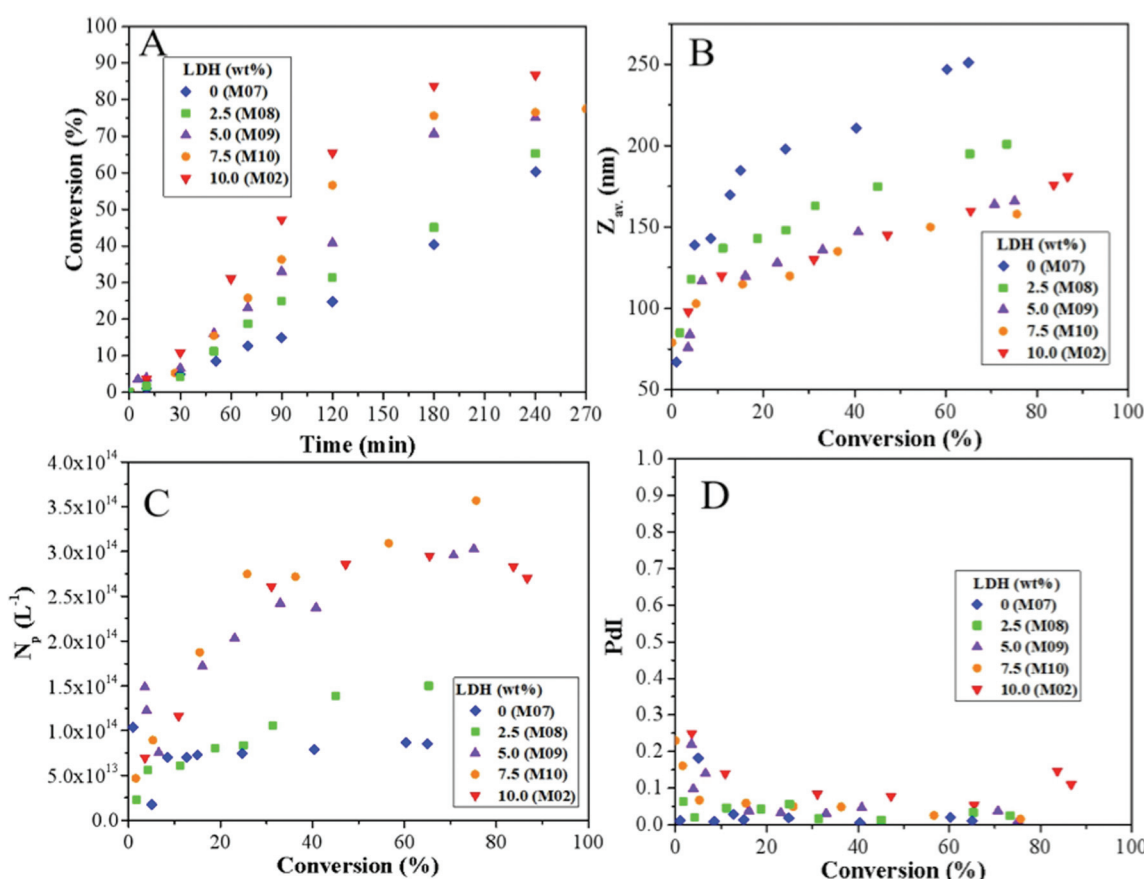


Fig. 10 Effect of LDH content on the evolutions of (A) the overall monomer conversion with time, and of (B) the average particle size ( $Z_{av}$ ), (C) the particle number ( $N_p$ ) and (D) the size dispersity with monomer conversion during Pickering emulsion copolymerization of St and MMA (80/20 wt/wt). LDH content = 0, 2.5, 5.0, 7.5 and 10 wt% based on total monomer (see Table 3 for experimental details).

of polymerization rate. The present results thus clearly demonstrate that the use of MMA as auxiliary comonomer can effectively promote LDH adsorption at the latex particle surface and reduce the total interfacial free energy of the system, making LDH platelets efficient solid stabilizers of Pickering emulsion polymerization of St.

Quite remarkably, the presence of LDH sheets covering the latex particles can be clearly identified on the high magnification image of Fig. 7. The platelets pave the surface in a more or less regular arrangement as a consequence of their high particle size distribution. Black “rods” corresponding to erected LDH sheets can also be seen at the polymer water interface. For geometric considerations, only the larger particles appear to be fully covered by LDH. Indeed, the LDH discs are too large to fully accommodate the high surface curvature of the smaller latex particles, resulting in average to only around 5 LDH platelets per latex particle (see Table 2). Such a low value again illustrates the capacity of the LDH sheets to efficiently stabilize the polymer latex particles.

**Effect of MMA content.** As MMA is also known to hydrolyze under basic conditions, we next wanted to determine to what extent increasing the amount of MMA could influence the outcome of the polymerization (Table 2). Fig. 8A shows the evolution of monomer conversion with time for increasing amounts of MMA and a fixed LDH content of 10 wt%.

The polymerization rate for pure St was very low and, as expected, increased significantly when a small amount of MMA (0.1 g, 10 wt% based on monomers, M01 in Table 2) was introduced in the monomer mixture. The polymerization rate increased further with increasing the MMA content from 0.1 to 0.3 g. However, when the latter exceeded the threshold value of 0.4 g (*i.e.*, 40 wt% based on total monomer, M04, M05 and M06 in Table 2), the system lost colloidal stability and completely coagulated. A similar behavior was reported by Teixeira *et al.*<sup>24</sup> during Pickering emulsion copolymerization of *n*-butyl acrylate and MMA using LAPONITE® clay as stabilizer, and was ascribed to *in situ* MMA hydrolysis. The deleterious effect of a too high concentration of the auxiliary comonomer was also emphasized by Li *et al.*<sup>29</sup> during the synthesis of IO-armored latexes. As shown in Fig. 8, the DLS particle size ( $Z_{av.}$ ) and the size distribution (indicated by the PDI value) were also strongly dependent on the MMA content and both decreased with increasing the amount of MMA at a given conversion, while the particle number concurrently increased, accounting for the higher reaction rate. It is worth mentioning here that contrary to the above HEMA experiments, DLS and TEM analyses were in reasonable good agreement for up to 20 wt% of MMA, and only began to diverge for 30 wt% of MMA (M03 in Table 2) suggesting again limited colloidal stability of the final latex particles. Latex destabilization was also evident in the kinetics analysis that revealed a sudden increase of both the particle size and the size dispersity by the end of the reaction

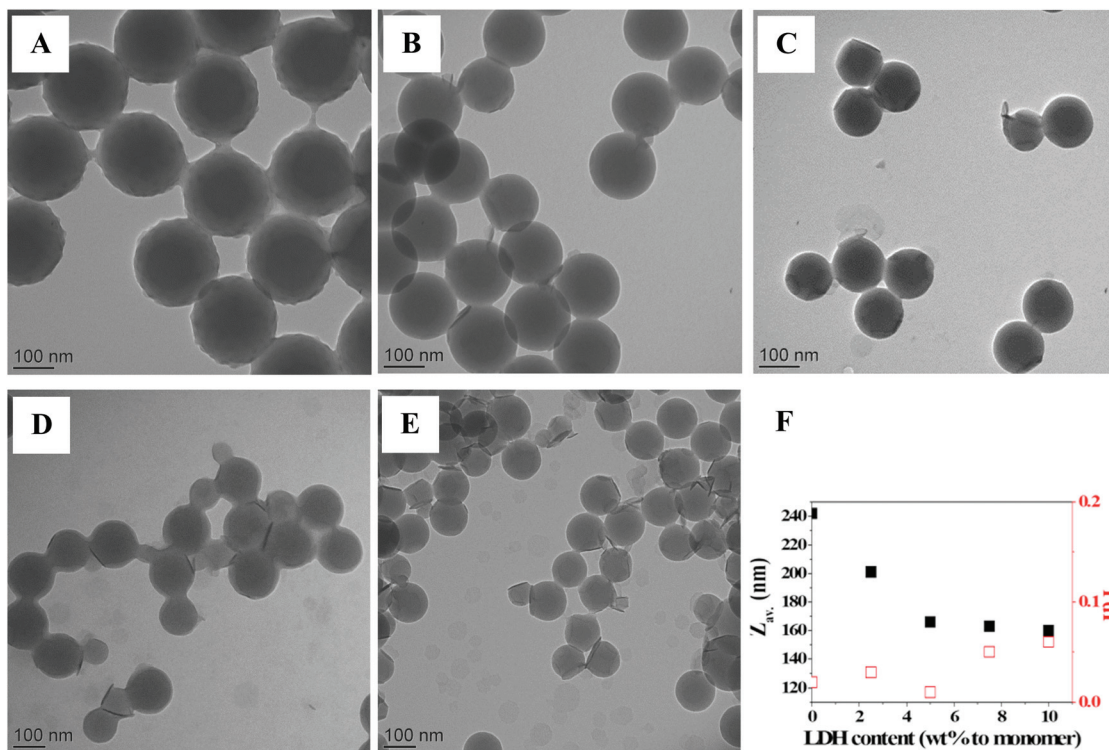


Fig. 11 TEM images of LDH/polymer composite latex particles obtained by Pickering emulsion copolymerization of St and MMA (80/20 wt/wt) for increasing LDH contents. (A) No LDH, (B) 2.5 wt%, (C) 5.0 wt%, (D) 7.5 wt% and (E) 10 wt% of LDH, based on total monomer (see Table 3 for details). (F) Average particle diameter and size dispersity determined by DLS vs. LDH content.



(orange circles in Fig. 8B and D). This last result is in line with the above observation of latex destabilization for 40 wt% of MMA, and confirms that the latter has a negative impact when it is used in too high relative proportions. As mentioned above, this can likely be attributed to MMA hydrolysis under basic conditions, and the release of MAA as attested by the gradual decrease of pH with increasing MMA content (Fig. S4, ESI†). As shown in Table 2 and Fig. 9, stable LDH-armored latexes with small particle sizes were however obtained for 10 and 20 wt% of MMA in the presence of 10 wt% of LDH.

**Effect of LDH content.** The influence of the LDH content on the diameter of the final latex particles and the polymerization kinetics was last evaluated for 20 wt% of MMA (Table 3 and Fig. 10). It was shown previously that the particle size was little influenced by the total amount of LDH introduced when HEMA was used as auxiliary comonomer (likely due to the concomitant destabilization of the LDH platelets), while the reaction rate increased. Herein, we carried out a series of copolymerization of St and MMA by varying the LDH content from 0 to 10 wt%. The reaction rate again increased with increasing the amount of LDH (Fig. 10A) due to the increased number of reaction loci, while the particle diameter decreased from 242

to 166 nm for up to 5 wt% of LDH and then stabilized for higher concentrations (Fig. 10B and 11). Besides, in contrast to HEMA, all latexes were stable with no sign of coagulation, each composite particle being surrounded by in average 4–5 LDH platelets, even though the size dispersity (determined by DLS or TEM) slightly increased with increasing LDH content.

Such a decrease in particle size with increasing the amount of Pickering stabilizer is an expected outcome of Pickering emulsion polymerization. However, it has not always been observed experimentally.<sup>25,53</sup> In particular, several authors have shown a diminution of the particle size down to a limiting value with a concomitant increase of the particle size distribution suggesting a longer nucleation period.<sup>22,24</sup> The plateauing of the particle size and the broadening of the particle size distribution with increasing LDH content, both indicate that a similar scenario is likely at play here. Additional information about the nucleation mechanism can be obtained by looking at the evolution of the particle number with monomer conversion. While in the absence of LDH, the particle number was fixed at a relatively low conversion (<10%, M01, Fig. 10C), in the presence of LDH, the particle number steadily increased up to around 30% monomer conversion and then leveled off

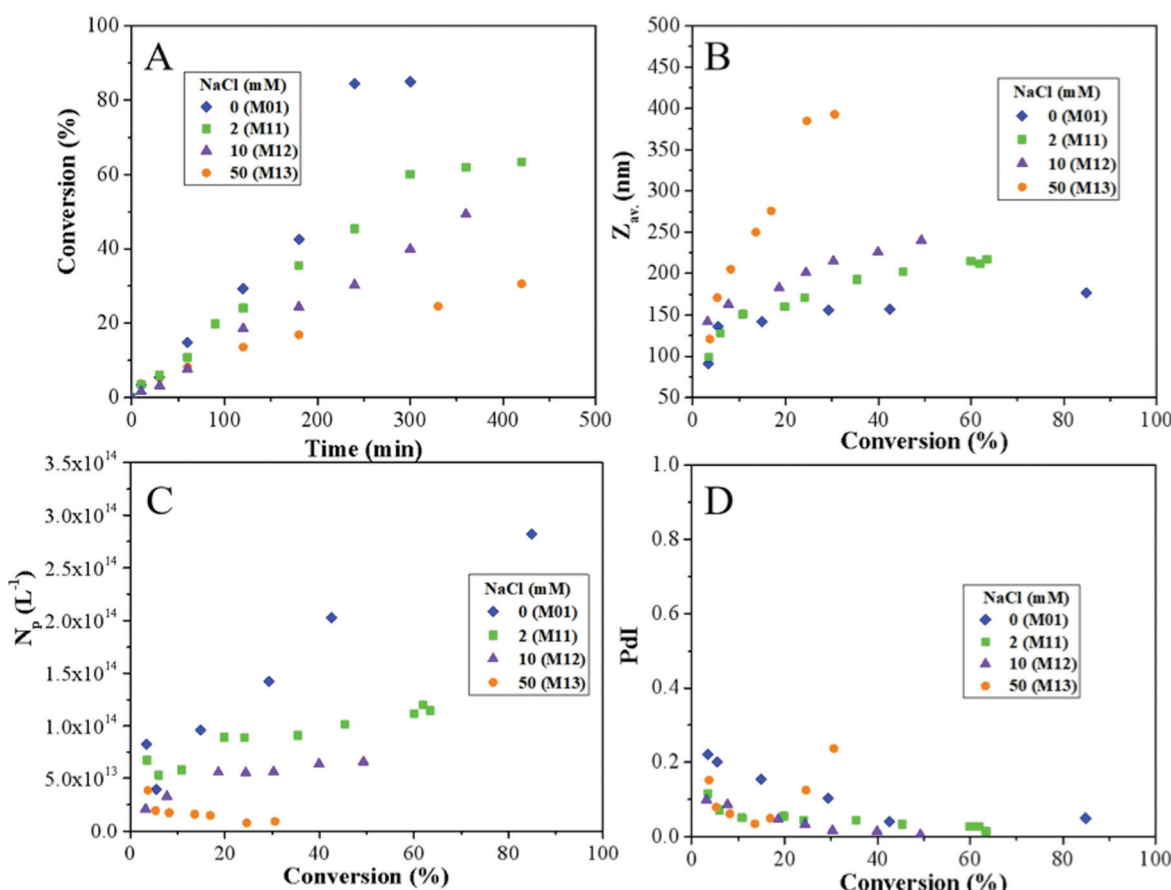


**Fig. 12** Effect of the NaCl concentration on the evolutions of (A) the overall monomer conversion with time, and of (B) the average particle size ( $Z_{av}$ ), (C) the particle number ( $N_p$ ) and (D) the size dispersity ( $Pdl$ ) with conversion during Pickering emulsion copolymerization of St and MMA (90/10 wt/wt) in the presence of 10 wt% of LDH (based on total monomer).  $[\text{NaCl}] = 0, 2, 10$  and  $50 \text{ mM}$  (see Table 4 for experimental details).



indicating slow nucleation. To go one step further, we have plotted in Fig. S5 (ESI†) the evolution of the latex diameter ( $D$ ) versus the cube root of monomer conversion. As the particle number scales to  $D^3$ , a constant particle number should lead to a straight line. This was indeed the case for M07 but the plots showed deviation from the linear fit for all experiments performed in the presence of LDH. The deviation was more pronounced for high LDH contents, indicating that the higher the amount of LDH, the more prolonged was the nucleation period.

**Effect of ionic strength.** Another important parameter that is known to influence the formation and the stability of Pickering latexes is the ionic strength. Salts are well known for screening electrostatic repulsions and promote interfacial adsorption.<sup>54</sup> For instance, Yang *et al.*<sup>41</sup> have investigated the effect of salt on the formation and stability of LDH Pickering emulsions and concluded that the presence of salt caused an increase in the hydrophobicity of the LDH platelets promoting their adsorption at the oil/water interface. The copolymerization of St and MMA (St/MMA = 90/10 wt/wt) was thus investigated in the presence of 10 wt% of LDH and increasing amounts of NaCl chosen as inert salt, covering a wide range of concentrations from 2 to 50 mM (Table 4 and Fig. 12).

As shown in Table 4 and in Fig. 12A and B, the DLS particle size increased by more than a factor two (from 177 to 385 nm) when the NaCl concentration was increased from 0 to 50 mM, while the polymerization rate concomitantly decreased indicating that the addition of salt compressed the double layer and reduced electrostatic repulsions at the surface of the LDH-armored latexes, resulting in the formation of larger particles. A significant increase of the particle size and high PDI were observed for 50 mM NaCl, indicating that as expected, too high an ionic strength promoted latex aggregation. Indeed, the resulting latex became unstable after 24 hours and completely coagulated.

The TEM micrographs displayed in Fig. 13 confirmed the armored morphology and the DLS results. Although more LDH platelets were apparently adsorbed on the latex particles (the platelets appear to be more closely packed on the surface likely due to lower electrostatic repulsions between adjacent LDH sheets), the TEM images also suggest that there is more free LDH in water for high than for low salt concentrations, which may be due to two concomitant effects: (i) the decrease of the total surface area of the latex particles as the salt concentration increases and (ii) LDH aggregation in water prior to their adsorption on the latex particle surface.

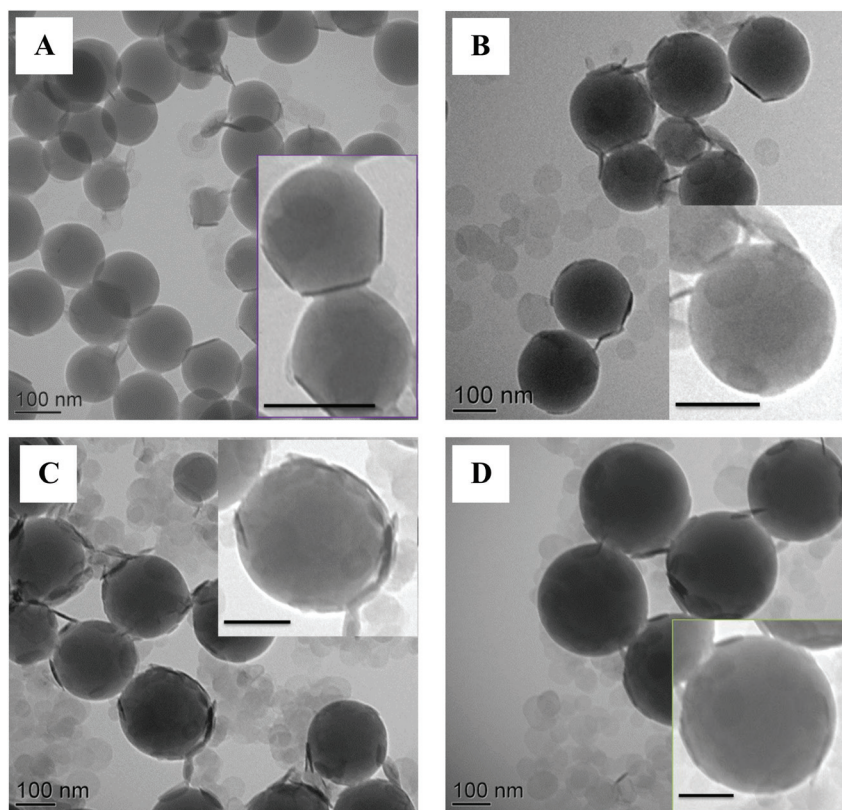


**Fig. 13** TEM images of LDH/polymer composite latex particles obtained by Pickering emulsion copolymerization of St and MMA (90/10 wt/wt) for increasing NaCl concentrations and 10 wt% of LDH. (A) No salt, (B) [NaCl] = 2 mM, (C) [NaCl] = 10 mM and (D) [NaCl] = 50 mM (runs M01, M11, M12 and M13 in Table 4). Scale bar = 100 nm.



## Conclusions

LDH-armored latex particles have been synthesized through surfactant-free emulsion polymerization of St using HEMA and MMA as auxiliary comonomers. Adsorption of the LDH platelets on the polymer particle surface was promoted by *in situ* hydrolysis of the functional comonomers (which is known to occur in alkaline conditions), leading to the formation of an alcohol molecule and MAA. Under our experimental conditions (pH = 10.2), the carboxylic acid group is fully dissociated resulting in *in situ* electrostatic interactions of the growing oligoradicals with the positively charged LDH platelets, promoting subsequent LDH adhesion to the latex particle surface. Composite latexes with the targeted armored morphology were indeed successfully obtained for both comonomers, in a one-step process (*i.e.* no pretreatment of the LDH surface was required). We showed that a too high amount of HEMA, which is fully water soluble, induced colloidal instabilities likely due to the too high concentration of released MAA. Stable LDH-armored latexes could be however successfully obtained for 8 wt% of HEMA (based on total monomer) and 10 wt% of LDH. Similar results were observed for MMA although destabilization occurred at a much higher concentration of 30 wt%. In both cases, the reaction rate increased with increasing the amount of auxiliary comonomer or the LDH content due to the concomitant increase of the number of nucleation loci. While in the case of HEMA, the particle size was barely influenced by the amount of LDH, the diameter of the LDH-armored particles synthesized in the presence of MMA, decreased by almost a factor 2 when the amount of Pickering stabilizer was increased from 0 to 7.5 wt% and leveled off for higher LDH contents. This led to latex particles with a diameter as low as 122 nm surrounded by in average 5 LDH sheets, emphasizing the high stabilizing efficiency of the LDH platelets that can be attributed to their high surface charge density. Finally, we showed that the addition of salts screened the LDH surface charges and electrostatic repulsions between adsorbed platelets, resulting in the formation of larger particles with a higher LDH packing density. The resulting LDH-armored particles could be potentially assembled into superstructures and film materials with advantageous properties for a wide range of applications that can benefit from the incorporation of a rigid LDH phase. The synthesis of such film-forming particles and the study of their properties is a topic that we would like to address in future works.

## Conflicts of interest

There is no conflict of interest.

## Acknowledgements

Financial support from ANR-11-JS08-0013 (PolyHydRAFT) is gratefully acknowledged.

## References

- 1 J. L. Keddie and A. F. Routh, Surfactant distribution in latex films, in *Fundamentals of latex film formation*, Springer, Dordrecht, 2010.
- 2 P. B. Zetterlund, S. C. Thickett, S. Perrier, M. Lansalot and E. Bourgeat-Lami, *Chem. Rev.*, 2015, **115**, 9745–9800.
- 3 A. Schrade, K. Landfester and U. Ziener, *Chem. Soc. Rev.*, 2013, **42**, 6823–6839.
- 4 E. Bourgeat-Lami, N. Sheibat-Othman and A. M. Dos Santos, in *Polymer Nanocomposites by Emulsion and Suspension Polymerization*, The Royal Society of Chemistry, 2011, ch. 13, pp. 269–311.
- 5 W. Ramsden, *Proc. R. Soc. London*, 1903, **72**, 156–164.
- 6 S. U. Pickering, *J. Chem. Soc. Trans.*, 1907, **91**, 2001–2021.
- 7 I. Martín-Fabiani, M. L. Koh, F. Dalmas, K. L. Elidottir, S. J. Hinder, I. Jurewicz, M. Lansalot, E. Bourgeat-Lami and J. L. Keddie, *ACS Appl. Nano Mater.*, 2018, **1**, 3956–3968.
- 8 J. Faucheu, C. Gauthier, L. Chazeau, J.-Y. Cavaille, V. Mellon and E. Bourgeat-Lami, *Polymer*, 2010, **51**, 6–17.
- 9 L. Delafresnaye, P.-Y. Dugas, P.-E. Dufils, I. Chaduc, J. Vinas, M. Lansalot and E. Bourgeat-Lami, *Polym. Chem.*, 2017, **8**, 6217–6232.
- 10 N. Negrete-Herrera, J.-L. Putaux, L. David, F. De Haas and E. Bourgeat-Lami, *Macromol. Rapid Commun.*, 2007, **28**, 1567–1573.
- 11 T. Wang, P. J. Colver, S. A. F. Bon and J. L. Keddie, *Soft Matter*, 2009, **5**, 3842.
- 12 R. Ruggerone, C. J. G. Plummer, N. N. Herrera, E. Bourgeat-Lami and J.-A. E. Manson, *Eur. Polym. J.*, 2009, **45**, 621–629.
- 13 R. Ruggerone, C. J. G. Plummer, N. N. Herrera, E. Bourgeat-Lami, J.-A. E. Manson and E. Kny, *Solid State Phenom.*, 2009, **151**, 30–34.
- 14 N. Zgheib, J.-L. Putaux, A. Thill, F. D'Agosto, M. Lansalot and E. Bourgeat-Lami, *Langmuir*, 2012, **28**, 6163–6174.
- 15 H. Zhu, L. Lei, B.-G. Li and S. Zhu, Development of Novel Materials from Polymerization of Pickering Emulsion Templates, in *Polymer Reaction Engineering of Dispersed Systems: Volume I*, ed. W. Pauer, Springer International Publishing, Cham, 2018, pp. 101–119.
- 16 M. J. Percy, C. Barthet, J. C. Lobb, M. A. Khan, S. F. Lascelles, M. Vamvakaki and S. P. Armes, *Langmuir*, 2000, **16**, 6913–6920.
- 17 J. I. Amalvy, M. J. Percy, S. P. Armes and H. Wiese, *Langmuir*, 2001, **17**, 4770–4778.
- 18 M. Chen, L. Wu, S. Zhou and B. You, *Macromolecules*, 2004, **37**, 9613–9619.
- 19 M. Chen, S. Zhou, B. You and L. Wu, *Macromolecules*, 2005, **38**, 6411–6417.
- 20 D. Dupin, A. Schmid, J. A. Balmer and S. P. Armes, *Langmuir*, 2007, **23**, 11812–11818.
- 21 N. Sheibat-Othman and E. Bourgeat-Lami, *Langmuir*, 2009, **25**, 10121–10133.
- 22 A. Lotierzo and S. A. F. Bon, *Polym. Chem.*, 2017, **8**, 5100–5111.



23 E. Bourgeat-Lami, T. R. Guimaraes, A. M. C. Pereira, G. M. Alves, J. C. Moreira, J.-L. Putaux and A. M. dos Santos, *Macromol. Rapid Commun.*, 2010, **31**, 1874–1880.

24 R. F. A. Teixeira, H. S. McKenzie, A. A. Boyd and S. A. F. Bon, *Macromolecules*, 2011, **44**, 7415–7422.

25 N. Sheibat-Othman, A.-M. Cenacchi-Pereira, A. M. Dos Santos and E. Bourgeat-Lami, *J. Polym. Sci., Part A: Polym. Chem.*, 2011, **49**, 4771–4784.

26 B. Brunier, N. Sheibat-Othman, M. Chniguir, Y. Chevalier and E. Bourgeat-Lami, *Langmuir*, 2016, **32**, 6046–6057.

27 B. Brunier, N. Sheibat-Othman, Y. Chevalier and E. Bourgeat-Lami, *Langmuir*, 2016, **32**, 112–124.

28 Z. Xu, A. Xia, C. Wang, W. Yang and S. Fu, *Mater. Chem. Phys.*, 2007, **103**, 494–499.

29 K. Li, P. Y. Dugas, M. Lansalot and E. Bourgeat-Lami, *Macromolecules*, 2016, **49**, 7609–7624.

30 J. H. Chen, C.-Y. Cheng, W.-Y. Chiu, C.-F. Lee and N.-Y. Liang, *Eur. Polym. J.*, 2008, **44**, 3271–3279.

31 J. Jeng, T.-Y. Chen, C.-F. Lee, N.-Y. Liang and W.-Y. Chiu, *Polymer*, 2008, **49**, 3265–3271.

32 X. Song, G. Yin, Y. Zhao, H. Wang and Q. Du, *J. Polym. Sci., Part A: Polym. Chem.*, 2009, **47**, 5728–5736.

33 X. Song, Y. Zhao, H. Wang and Q. Du, *Langmuir*, 2009, **25**, 4443–4449.

34 Z. Yongliang, Y. Guannan, Z. Zheng, W. Haitao and D. Qiangguo, *J. Polym. Sci., Part A: Polym. Chem.*, 2011, **49**, 5257–5269.

35 G. Yin, Z. Zheng, H. Wang and Q. Du, *J. Colloid Interface Sci.*, 2011, **361**, 456–464.

36 Q. Wang and D. O'Hare, *Chem. Rev.*, 2012, **112**, 4124–4155.

37 C. Taviot-Guého, V. Prévot, C. Forano, G. Renaudin, C. Mousty and F. Leroux, *Adv. Funct. Mater.*, 2018, **28**, 1703868.

38 V. Prevot and E. Bourgeat-Lami, Recent advances in layered double hydroxide/polymer latex nanocomposites: from assembly to in situ formation, in *Layered Double Hydroxide Polymer Nanocomposites*, ed. T. Sabu and D. Saju, Woodhead Publishing, 2020, ch. 11, pp. 461–495.

39 Y. Liu, Y. Gao, Q. Wang and W. Lin, *Dalton Trans.*, 2018, **47**, 14827–14840.

40 L. Yan, S. Gonca, G. Zhu, W. Zhang and X. Chen, *J. Mater. Chem. B*, 2019, **7**, 5583–5601.

41 F. Yang, S. Liu, J. Xu, Q. Lan, F. Wei and D. Sun, *J. Colloid Interface Sci.*, 2006, **302**, 159–169.

42 Y. Shan, C. Yu, J. Yang, Q. Dong, X. Fan and J. Qiu, *ACS Appl. Mater. Interfaces*, 2015, **7**, 12203–12209.

43 N. Zhang, L. Zhang and D. Sun, *Langmuir*, 2015, **31**, 4619–4626.

44 G. Li, Z. Song, W. Liu, D. Yu and H. Wang, *Ind. Eng. Chem. Res.*, 2017, **56**, 11435–11442.

45 L. Qiu and B. Qu, *J. Colloid Interface Sci.*, 2006, **301**, 347–351.

46 S. Pearson, M. Pavlovic, T. Augé, V. Torregrossa, I. Szilagyi, F. D'Agosto, M. Lansalot, E. Bourgeat-Lami and V. Prévot, *Macromolecules*, 2018, **51**, 3953–3966.

47 C. Forano, U. Costantino, V. Prevot and C. Taviot Gueho, in *Developments in Clay Science*, ed. F. Bergaya and G. Lagaly, Elsevier, 2nd edn, 2013, ch. 14.1, pp. 745–782.

48 O. A. Kazantsev, K. V. Shirshin, A. P. Sivokhin, S. V. Tel'nov, I. V. Zhiganov, A. E. Kuznetsov and Y. L. Mironycheva, *Russ. J. Appl. Chem.*, 2003, **76**, 1296–1298.

49 O. A. Kazantsev, D. V. Orekhov, A. P. Sivokhin, D. M. Kamorin and M. V. Savinova, *Des. Monomers Polym.*, 2017, **20**, 136–143.

50 F. Kovanda, E. Jindová, K. Lang, P. Kubát and Z. Sedláková, *Appl. Clay Sci.*, 2010, **48**, 260–270.

51 B. A. Robinson and J. W. Tester, *Int. J. Chem. Kinet.*, 1990, **22**, 431–448.

52 C. A. Colard, R. F. Teixeira and S. A. Bon, *Langmuir*, 2010, **26**, 7915–7921.

53 P. J. Colver, C. A. L. Colard and S. A. P. Bon, *J. Am. Chem. Soc.*, 2008, **130**, 16850–16851.

54 S. Cauvin, P. J. Colver and S. A. F. Bon, *Macromolecules*, 2005, **38**, 7887–7889.

